# Accepted Manuscript


Experimental determination of the static and fatigue strength of the adhesive joints bonded by epoxy adhesive including different particles

İsmail Saraç, Hamit Adin, Şemsettin Temiz

PII: S1359-8368(18)31464-1

DOI: 10.1016/j.compositesb.2018.08.006

Reference: JCOMB 5836

To appear in: *Composites Part B*

Received Date: 11 May 2018

Revised Date: 16 July 2018

Accepted Date: 2 August 2018

Please cite this article as: Saraç İ, Adin H, Temiz Ş, Experimental determination of the static and fatigue strength of the adhesive joints bonded by epoxy adhesive including different particles, *Composites Part B* (2018), doi: 10.1016/j.compositesb.2018.08.006.

**Graphical Abstract**

Single lap joints geometry and dimensions

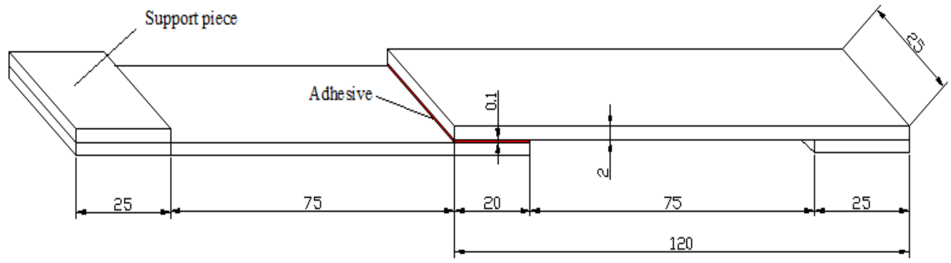


The schematic diagram of the fixture

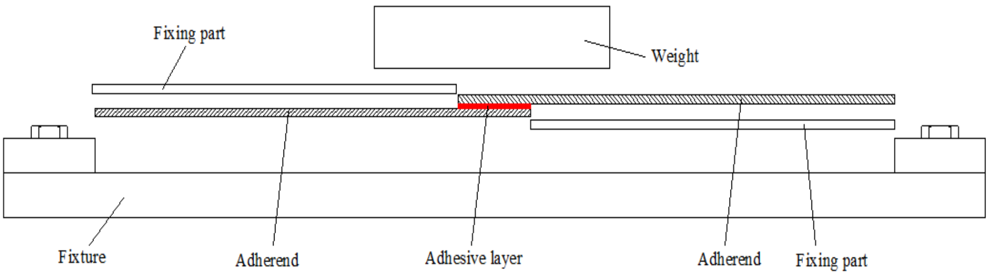


100 kN computer controlled Shimadzu EHF-EV universal fatigue device

Load-displacement curves of the joints

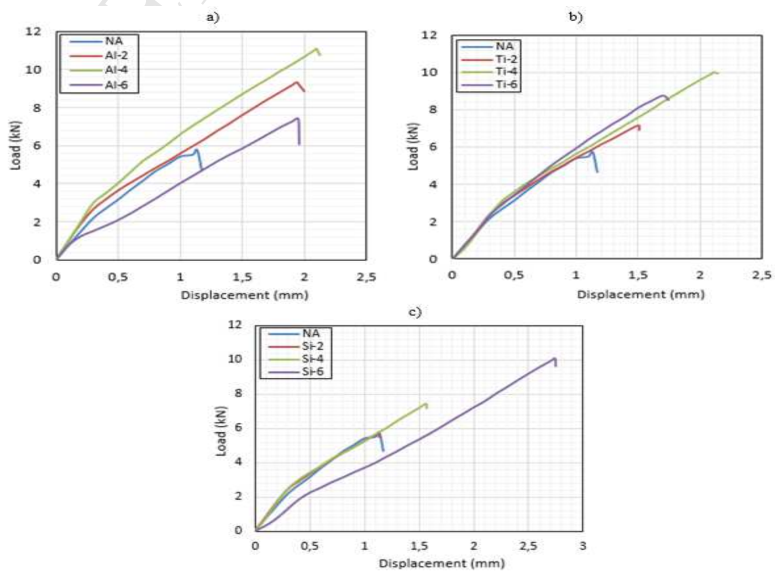

Fracture surfaces of the SLJs (a-unreinforced, b-reinforced by $Al_2O_3$, c-reinforced by $TiO_2$, d- reinforced by $SiO_2$)

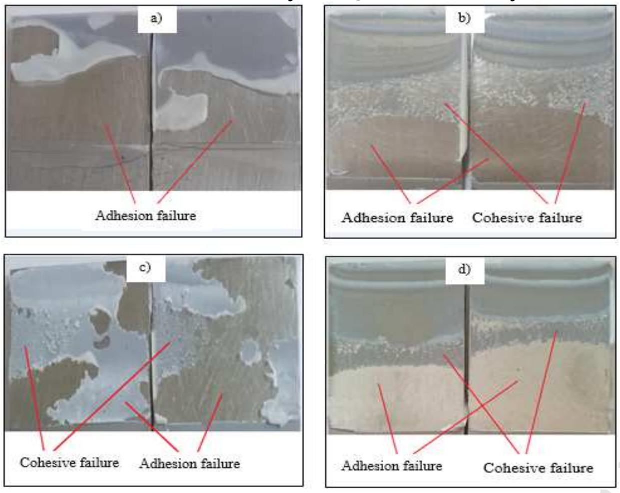

# Experimental determination of the static and fatigue strength of the adhesive joints bonded by epoxy adhesive including different particles

İsmail Saraç[a], Hamit Adin [a,*] Şemsettin Temiz[b]
[a]*Department of Mechanical Engineering, Batman University, Batman, 72060, Turkey*
[b]*Department of Mechanical Engineering, Inonu University, Malatya, 44120, Turkey*

**ABSTRACT:**
Because of their many advantages, adhesively bonded joints are intensively used in many engineering fields. So, the mechanical research of the adhesively bonded joints is very important to use these joints safely. There are many studies performed by researchers to investigate the mechanical properties of the adhesive joints. There has been a considerable interest in nanoparticles added to structural adhesives recently because nanoparticles improve the mechanical properties of adhesives and joints. In this paper, different nanoparticles reinforced by epoxy adhesive, and neat adhesive were used to produce single lap joints. The static and fatigue strengths of single lap joints incorporating nanoparticles were compared to those without nanoparticles. Experiments were performed at 20 mm overlap length. DP460 epoxy was used as the adhesive material, and nano-$Al_2O_3$, nano-$TiO_2$ and nano-$SiO_2$ were used as the nanoparticles; and AISI 304 stainless steel plates were used as the adherents. The results of the experimental research revealed that average failure load increased significantly in nanoparticle-reinforced adhesive joints. The highest average failure load was obtained with 4wt% nano-$Al_2O_3$ in epoxy adhesive. Fatigue tests were performed at 10 Hz frequency, and 0.1 loading ratio (R). When the fatigue test results were examined, it was observed that the addition of the nano-$Al_2O_3$ and nano-$SiO_2$ to the adhesive increased fatigue strength of the adhesive joints, on the other hand, the addition of the nano-$TiO_2$ to the adhesive reduced fatigue strength of the adhesive joints.

**Key words:** A. Adhesion B. Single lap joints C. Particle-reinforcement D. Strength E. Fatigue

## 1. Introduction

It is a rare occurrence that structures and modern engineering components are subjected to static loading only. The vast majority of parts in structures are subjected to regular or irregular cyclic loads. For this reason, design analysts focus on the failures that develop due to cyclic loads in materials. In structural components exposed to cyclic loads, regular/irregular repetitive stresses occur based on loading type, and these stresses usually cause the component to fail due to fatigue [1].

With the development of adhesive technology after the Second World War, the use of adhesively bonded joints has increased significantly. For this reason, fatigue of adhesive joints has emerged as an important research field. Especially, after the 1970s, the increase in use of adhesive joints in the aerospace industry has increased the importance of fatigue analyzes further.

It is known that the fatigue event develops due to a number of defects and discontinuities in materials and causes damage in materials. Thus, there is always a possibility of bonding of adhesive joints at the bonding area, or in the adhesive layer. These defects, which are not visible, cause fatigue damage when subjected to cyclic loading with time. Therefore, in addition to determining the mechanical properties of adhesive joints under static loads, it is also vital to determine their fatigue behavior under cyclic loads. Mechanical parts are usually exposed to dynamic and cyclic loads. Such parts subjected to cyclic loads may experience fatigue failure in time under stress values below their static strength. So, it is important to determine the fatigue strength of the adhesive joints in all its aspects.

While investigating the static and fatigue strengths of adhesive joints, studies on the overlap length, adherent thickness, adhesive thickness, geometry of joint, loading forms (constant amplitude, variable amplitude), loading rate (R), frequency, surface operations, temperature and environmental conditions such as humidity, composite patch, hybrid joint, etc. were carried out on the subject[2-7].

Recently, there have been some studies as noted below in the literature concerning the effect of various nanoparticles, particularly those incorporated in epoxy adhesives, on the mechanical properties of the adhesive joints [8-11]. When these studies are examined; it can be seen that nanoparticles have an important effect on the mechanical properties of the adhesive joints. As seen in these studies, nanoparticles improve the properties of the adhesive, despite the use of small amount in the adhesives. Nanoparticles; while contributing positively to thermal, electrical and thermos-mechanical properties of adhesives, nanoparticles also increase the durability of adhesives against environmental factors, and equip them with high water absorber properties, and improve their aging properties at the same time.

Meguid et al. [12] investigated the effect of nanoparticles added in the epoxy adhesive on the static strength of the adhesive joints. In the study, carbon fiber and epoxy resin laminate substrate and 6061-T6 aluminum substrate were used as adherents; and Dexter Hysol EA 9330 epoxy was used as the adhesive; and carbon nanotube (CNT), aluminum nano-powder (ANP) were used as the nanoparticles. The results showed that varying the weight percentage of the nanoparticles into the epoxy adhesive considerably influences the debonding and shear characteristics of the interface. The results also showed that increasing the amount of the nanoparticles beyond a certain weight fraction of the adhesive decreases the interface strength.

Zhai et al. [13] studied the influence of different nanoparticles and surface roughness on the adhesion between epoxy adhesive and substrate. In the study, steel sheets were used to be the adherent, epoxy adhesive of Pattex® Kraft-Mix adhesive (Henkel Adhesives Ltd.), a two-component system was used as the adhesive; and nano-$Al_2O_3$, nano-$CaCO_3$ and nano-$SiO_2$ were used as the nanoparticles. The results of pull-off adhesion tests showed that nano-$Al_2O_3$ of the three kinds of nanoparticles had the most influence on adhesion strength. As the results showed that modified by 2% nano-$Al_2O_3$, the adhesion strength of epoxy adhesive on the surface abraded with 150# was visibly improved by about 5 times.

In a study performed by Srivastava [14], carbon/carbon–silicon carbide (C/C–SiC) composite was produced. Multiwall carbon nanotubes (MWCNTs) filled and unfilled epoxy resin were used for bonding of composite substrates. The test results indicated that 3% MWCNT filled epoxy resin bonded C/C–C/C and C/C–SiC–C/C–SiC substrates had a higher adhesive joint strength than those bonded with epoxy resin alone.

In a study conducted by Mactabi et al. [15], aluminum single lap joints were produced, using carbon nanotube reinforced epoxy adhesive, and the electrical resistance case of the joints was monitored during fatigue loading. The conductive network was obtained by carbon nanotube reinforcement inside the adhesive. This study indicated an in situ monitoring technique which is promising in evaluating the integrity and predicting the residual life of adhesively bonded single lap joints subjected to fatigue loading.

In a study done by Kang et al. [16], the static and dynamic strengths of adhesive joints reinforced by carbon nanotubes were compared to those of adhesive joints without carbon nanotubes. Composite aluminum single-lap joints were produced, and their strengths were examined. The test results showed that fatigue strength of the adhesive joints reinforced by carbon nanotubes increased, in contrast to this, the static strength of the adhesive joints reinforced by carbon nanotubes decreased.

In a study performed by Khashaba et al. [17], scarf adhesive joints (SAJs) with $5^0$ and $10^0$ scarf angles were manufactured. Carbon fiber composite adherents and epoxy adhesive reinforced by nano-SiC and nano-$Al_2O_3$ were used to manufacture SAJs. The test results showed that the ultimate tensile strengths of $5^0$ and $10^0$ SAJs were respectively improved by 41.2% and 8.4% for SiC/E-SAJs and 22.5% and 26.5% for $Al_2O_3$-SAJ compared to neat epoxy-SAJs.

In a study conducted by Akpınar [18], the mechanical properties of single lap joints reinforced by nano-$Al_2O_3$ and nano-$TiO_2$ nanoparticles were investigated. When the results obtained from the experiments were examined; it was seen that the tensile failure load increased with the use of nanoparticle-added adhesives. Furthermore, when the force-displacement curves of the joints were examined, it was determined that the displacement capacities of the adhesive joints reinforced by nanoparticles also increased.

In a study done by Khashaba et al. [19], the fatigue performance of scarf adhesive joints (SAJs) reinforced by multi-walled carbon nanotubes (MWCNTs), nano-SiC and nano-$Al_2O_3$ was investigated. The scarf adhesive joints (SAJs) were subjected to uniaxial static tensile and constant amplitude fatigue loading. Results from fatigue tests showed that the fatigue lives of the modified SAJs with MWCNTs and SiC increased, while the fatigue lives of the modified $Al_2O_3$ decreased.

In the study performed by Akpınar et al. [20], nanoparticles were added to the adhesive to increase the damage load of the adhesive joints and tensile and bending moment damage loads of these joints were experimentally investigated. The test results indicated that the addition of nanoparticles to the adhesive increased the tensile and four-point bending damage load of joint.

In the study performed by Razavi et al. [21], the average shear strength and elongation at failure of adhesively bonded single lap joints obtained using nanoparticle reinforced adhesive were studied. Different mixtures of two nanoparticles i.e. silica nanoparticles and multi walled carbon nanotubes were added to the adhesive. The experimental results demonstrated that adding the mixed nanoparticles had a significant effect on the mechanical behavior of single lap joints.

The aim of this work is to improve the mechanical properties of adhesive joints by adding nanoparticles to the adhesive. In this study, nano-$Al_2O_3$, nano-$TiO_2$ and nano-$SiO_2$ powders were added to the epoxy adhesive to produce nanoparticle reinforced adhesive joints, and unreinforced adhesive joints were produced to compare static and fatigue strengths of the single lap joints experimentally.

## 2. Experimental work

### *2.1. Materials*

In the experimental work, AISI 304 stainless steel sheet with a thickness of 2 mm was used as an adherent material. For bonding, a two part DP460 epoxy adhesive produced by 3M Company (St. Paul, MN, USA), was used as adhesive. For the nanoparticles in the adhesive, $Al_2O_3$, $TiO_2$ and $SiO_2$ nanoparticles (Nanografi, Ankara, Turkey) having an average size of 15-20 nm were used. Mechanical properties for the adhesive and adherent used in the experimental study are given in Table 1 and Table 2. The material properties of the nanoparticles are presented in Table 3.

**Table 1** Material properties of the adhesive [22].

**Table 2** Material properties of the adherend [23].

**Table 3** Properties of the nanoparticles [24].

DP460 Epoxy adhesive have different curing conditions. Curing condition used in this study, and mixing ratio of the DP460 Epoxy adhesive is given Table 4.

**Table 4** Curing condition and mixing ratio of the DP460 [25].

### *2.2. Manufacturing of the single lap joints (SLJs)*

#### *2.2.1. Providing surface preparation of the adherent*

AISI 304 stainless steel sheets with a thickness of 2 mm were cut by laser cutting method to produce single lap test specimens of 120 x 25 mm (Fig. 1). Surface preparation is essential for adhesively bonded joints to demonstrate high performance. The bonding surfaces were abraded with P80 grade emery paper to remove contaminants and to roughen. Then, these eroded surfaces were washed with powder detergent under tap water. After washing, bonding surfaces were cleaned by means of acetone, following this, bonding surfaces were flushed by tap water. Bonding surface conditioning procedures were finished by drying the adherents by means of heated air.

**Fig. 1.** Single lap joint geometry

#### *2.2.2. Preparation of adhesive materials*

In this study, the method used by Zhai et al. [13] was preferred to add nanoparticles into the adhesive because similar nanoparticles were used by Zhai et al. [13]; and stated this method's reliability and convenience. In this method, nanoparticles were directly added in epoxy adhesive and mechanically mixed with a spatula around 5 min. In Fig. 2, adhesive and nanoparticle weighing procedure previous to mixing was demonstrated. To make comparison, neat adhesive was also prepared.

**Fig. 2.** The determination of adhesive and nanoparticle weight

*2.2.3. Mounting of the single lap joints*

To manufacture tensile and fatigue test specimens of SLJs according to joint types, nanoparticle-reinforced or neat adhesives were applied on the bonding area as seen in Fig. 3 and the specimens were placed into the mold illustrated in Fig 4. The mold's schematic diagram was also illustrated in Fig. 5. Three specimens were manufactured in the mold at a time.

**Fig. 3.** The application of adhesive to adherents

**Fig. 4.** The mold used in the preparation of the SLJs samples

**Fig. 5.** Molding in the production of samples

Following this, in order to obtain a constant adhesive layer and to ensure that the adhesive is fully spread over the surfaces, pressure was applied on the bonding area by weights shown in Fig. 6. Pressure performed during bonding process increases the surface wetting ability of the adhesive and affects the adhesive thickness. The adhesive thickness recommended in the literature is 0.05-0.2 mm [26]. In the experiments made with various adhesives in the literature, the curing pressure was taken around 1 - 0.05 MPa [26]. In this study, curing pressure of 0.4 MPa was applied to the bonding area by means of weights placed on the bonding area. Since the pressure applied through the weight to the bonding area is constant in all samples, the bond line thickness is also constantly measured in all samples. As a result of the measurement of the adhesive thickness, the bonding line thickness of 0.4 MPa was calculated as 0.1 - 0.15 mm as a result of the curing pressure. In order to measure the adhesive layer thickness, the thicknesses of the parts to be bonded were measured separately using digital calipers before bonding. After the bonding process, the thickness of the bonding area was measured and the adhesive thickness was calculated by subtracting the thickness of the pieces to be adhered. This thickness is between the recommended values for the adhesive joints. The weights placed on the adhesive joints were taken away after 24 hours and the samples were removed from the mold as shown in Fig. 7. The specimens were allowed to cure completely for 7 days at room temperature and they were ready for experiments.

**Fig. 6.** Applying weight to samples

**Fig. 7.** The samples removed from the mold subsequent to curing process

*2.3. Mechanical testing of SLJs*

A series of mechanical test were carried out to determine the effects of $Al_2O_3$, $TiO_2$ and $SiO_2$ nanoparticles added in the adhesive on the tensile and fatigue properties of SLJs. The boundary conditions of the SLJs are shown in Fig. 8.

**Fig. 8.** The boundary conditions of the SLJs

*2.3.1. Tensile tests of the SLJs*

The tensile tests were performed with a Shimadzu AG-I 250 kN testing machine (Kyoto, Japan) (Fig.9) at ambient laboratory environment, under 1 mm/min crosshead speed. The sample types used in the tensile tests were shown in Table 5. Ten joint types were used to carry out the experiments. In order to increase the reliability of the test results, three samples were produced for each joint type, in total, 30 samples (10 joint type x 3: 30). The SLJs were carefully observed during tests and the maximum failure loads and ultimate tensile strains of SLJs were recorded. After the tests, the failure surfaces of samples were examined.

**Fig. 9.** Shimadzu AG-I (250 kN) tensile test device

**Table 5** Joint and particle types for fatigue tests

*2.3.2. Fatigue test of the SLJs*

The experiments were performed with a 100 kN computer controlled Shimadzu EHF-EV (Kyoto, Japan) universal fatigue device (Fig. 10) at ambient laboratory environment. All the fatigue tests were carried out under sinusoidal waveforms, constant load amplitude, frequency of 10 Hz, and stress ratio of 0.1. These test procedures are recommended by ASTM D3166 and used by some investigators [15,27]. To form the S-N curve, each type of the SAJs was tested at four different stress levels based on the average static strength. Fatigue run-out was determined as $10^7$ cycles. The sample types used in the fatigue experiments were shown in Table 6. Four joint types were used to carry out the experiments. The weight percentages of nanoparticles were used in this study selected according to the tensile test results, and performed in this study. In Table 7, the weight percentages used this study related to the maximum failure loads were shown. Therefore, at least five samples were tested for each stress level. 20 samples (4 stress levels x 5 experiment) were produced for each joint type, in total, 80 samples (4 joint type x 20: 80). The SLJs were carefully observed during fatigue tests and the number of cycles to failure of SLJs was recorded. After the tests, the failure surfaces of samples were examined.

**Fig. 10.** 100 kN computer controlled Shimadzu EHF-EV universal fatigue device

**Table 6** Joint types for fatigue tests
**Table 7** The maximum failure loads and the weight percentages of the nanoparticles

## 3. Results and discussion

*3.1. Tensile test results of the SLJs*

The experimental study was performed to investigate the effect of the nanoparticles added in the epoxy adhesive with different weight percentages (2%, 4%, 6%), on the mechanical properties involving the average failure loads and elongation at failure.

Fig. 11 illustrated the failure loads of the SLJs as a function of different weight percentages of nano-$Al_2O_3$, nano-$TiO_2$ and nano-$SiO_2$ in the adhesive. All the failure loads of reinforced joints were higher than unreinforced joints which were 5.28 kN, except the joints reinforced by 2% $SiO_2$. When the content was 4 wt% for $Al_2O_3$, the failure load was the highest, 10.42 kN, the failure load increased 97% compared to unreinforced joints. When the content was 4 wt% for $TiO_2$, the failure load was the highest, 9.87 kN, the failure load increased 86% compared to unreinforced joints. When the content was 6 wt% for $SiO_2$, the failure load was the highest, 10.09 kN, the failure load increased 91% compared to unreinforced joints.

**Fig. 11.** Average failure loads of the SLJs reinforced by nano-$Al_2O_3$, nano-$TiO_2$ and nano-$SiO_2$

Fig. 12 illustrated the load-displacement curves of the SLJs. When load-displacement curves were investigated, it was seen that nanoparticle reinforcement to the epoxy adhesive increased the displacement capacity of the SLJs. The displacement capacity of all the reinforced joints increased significantly compared to unreinforced joints. All the maximum failure loads of the joints were conformed to maximum displacement capacities of the joints. It can be said that nanoparticles added in the adhesive increases damage-damping capabilities and the displacement capacity of the joints and consequently the failure loads of the joints increase.

**Fig. 12.** Load-displacement curves of the joints

*3.2. Visual examination of failed joints*

The fracture surfaces of the failed adhesive joints are shown in Fig. 13. As it is seen in Fig. 13a, the failure of the unreinforced SLJs is interfacial. However, as shown in Fig. 13b-d, the failure mode of SLJs reinforced by nano-$Al_2O_3$, nano-TiO and nano-$SiO_2$ are a combination of cohesive and adhesive failures.

The active adhesive forces between the adherent and adhesive material and cohesive forces in the adhesive determine the strength of the joints. When the interfacial forces of interaction were exceeded due to the applied forces, an interfacial crack occurred and the adhesive–steel connection failed. Therefore, for unmodified joint system, failure was at the interfaces because these forces were weaker than the cohesive forces and did not stand the applied forces. However, for nano-modified joint system, the addition of nanoparticle may reinforce the interfacial forces in some way [28]. It can be said that epoxy adhesive has a strong interaction with steel substrate due to nanoparticles ($Al_2O_3$, $TiO_2$, $SiO_2$) used in this study.

Simple visual examination demonstrated differences in the fracture surfaces of nanoparticle reinforced joints and unreinforced joints. Namely, the single lap joints produced by nanoparticle reinforcement have bigger failure load than unreinforced joints, a larger bending moment is applied on the joint at higher failure load, and cracks improve from both ends of the overlap, producing symmetrical halves of the failed joints (as it is seen in Fig. 13 b,d). The mentioned bending moment above is based from the eccentricity of the single lap joints. The eccentricity of the joint introduces bending. Because of the bending, the peel stresses of the near ends of the joint can be large, causing joint failure.

**Fig. 13.** Fracture surfaces of the SLJs (a-unreinforced, b-reinforced by $Al_2O_3$, c-reinforced by $TiO_2$, d-reinforced by $SiO_2$)

*3.3. Fatigue test results of the SLJs*

In Fig. 14, the S-N curves of the SLJs are shown. As shown in Fig. 13, the endurance limit of adhesive joints increased with reinforcement nano-$Al_2O_3$ and nano-$SiO_2$, by contrast, with the endurance limit of adhesive joints decreased with reinforcement nano-$TiO_2$ as compared with unreinforced joints.

When Fig.14 was examined, the endurance limit of adhesive joints unreinforced was measured 2.37 kN, the endurance limit of adhesive joints reinforced by nano-$Al_2O_3$ was measured 2.90 kN, the endurance limit of adhesive joints reinforced by nano-$TiO_2$ was measured 1.85 kN, the endurance limit of adhesive joints reinforced by nano-$SiO_2$ was measured 2.64 kN. According to these results, nano-$Al_2O_3$ and nano-$SiO_2$ reinforcement increased the endurance limit of the joints by 22.3% and 11.3%, respectively. In contrary, nano-$TiO_2$ reinforcement decreased the endurance limit of the joints by 22%.

**Fig. 14.** S-N curves of the SLJs (a-reinforced by $Al_2O_3$/unreinforced, b-reinforced by $TiO_2$/unreinforced, c-reinforced by $SiO_2$/unreinforced)

In the experimental study performed by Kang et al. [16], so as to investigate why the fatigue strength of the adhesive joints with the carbon nanotubes increased, crack initiation and propagation of the adhesive joints were measured. Fig. 14 shows the crack length variation of adhesive joints with and without 2 wt% carbon nanotubes. As shown in Fig. 15, cracking of the adhesive joint without carbon nanotubes initiated at 1377 cycles and the fatigue fracture occurred simultaneously without any crack propagation time. However, the crack of the adhesive joint with carbon nanotubes initiated at 18,596 cycles and the fatigue fracture occurred at 26,297 cycles. From the test results of Fig. 15, it can be concluded that the fatigue life of the adhesive joint with carbon nanotubes is longer than that of the adhesive joint without carbon nanotubes because not only crack initiation but also crack propagation time are large when the carbon nanotubes are included in the adhesive layer. Similarly, in this study, the improving fatigue strength of the SLJs reinforced by nano-$Al_2O_3$ and $SiO_2$ can be related to this statement.

**Fig. 15.** Crack length variation of the adhesive joint [16].

*3.4. Visual examination of failed joints*

Fractured surfaces images were taken after fatigue tests of SLJs to investigate the fracture modes. Fig. 16-19 illustrate the fractured surfaces of the SLJs after fatigue tests. Simple visual examination demonstrated differences in the fracture surfaces of single lap joints tested at high and low maximum fatigue loads. It can be seen that at lower maximum loads, the area of interfacial failure increased. In contrast with this, it can be seen that at higher maximum loads, the area of cohesive failure increased generally.

**Fig.16.** Fractured surfaces of the SLJs produced with neat adhesive
(a-Pmax: 3,69 kN, b-Pmax: 3,17 kN, c-Pmax: 2,64 kN)

**Fig.17.** Fractured surfaces of the SLJs reinforced by nano-$Al_2O_3$
(a-$P_{max}$: 4,22 kN, b-$P_{max}$: 3,69 kN, c-$P_{max}$: 3,17 kN)

In a study performed by Khoramishad et al. [29], this is possibly due to the fact that as the damage evolution is slower in the low load case, there is a longer time for localized damage to take place during the longer cyclic life.

**Fig.18**. Fractured surfaces of the SLJs reinforced by nano-$TiO_2$
(a-$P_{max}$: 3,17 kN, b-$P_{max}$: 2,64 kN, c-$P_{max}$: 2,13 kN)

**Fig.19**. Fractured surfaces of the SLJs reinforced by nano-$SiO_2$
(a-$P_{max}$: 3,17 kN, b-$P_{max}$: 2,90 kN, c-$P_{max}$: 2,67 kN)

## 4. Conclusions and suggestions

The experimental study was performed to investigate the effect of the nanoparticles added in the epoxy adhesive on the mechanical properties involving the average failure load and fatigue strength in single lap-joint geometry.

The results obtained were as follows:

- All the failure loads of nanoparticle reinforced joints were higher than unreinforced joints which was 5.28 kN, except the joints reinforced by 2% $SiO_2$.
- When the content was 4 wt% for $Al_2O_3$, the highest failure load was obtained to be 10.42 kN, the failure load increased 97% compared to unreinforced joints. When the content was 4 wt% for $TiO_2$, the highest failure load was obtained to be 9.87 kN, the failure load increased 86% compared to unreinforced joints. When the content was 6 wt% for $SiO_2$, the highest failure load was obtained to be 10.09 kN, the failure load increased 91% compared to unreinforced joints.
- When load-displacement curves were investigated, it was seen that nanoparticle reinforcement to the epoxy adhesive increased the displacement capacity of the SLJs. The displacement capacity of all reinforced joints increased significantly compared to unreinforced joints.
- The failure mode of the unreinforced SLJs was obtained to be interfacial; the failure mode of SLJs reinforced by nano- $Al_2O_3$, nano-TiO and nano-$SiO_2$ was obtained to be a combination of cohesive and adhesive failures.
- After fatigue tests, it was seen that the endurance limit of adhesive joints increased with reinforcement nano-$Al_2O_3$ and nano-$SiO_2$, by contrast with this, the endurance limit of adhesive joints decreased with reinforcement nano-$TiO_2$ as compared with unreinforced joints.
- Nano-$Al_2O_3$ and nano-$SiO_2$ reinforcement increased the endurance limit of the joints 22.3% and 11.3%, respectively. In contrast with, nano-$TiO_2$ reinforcement decreased the endurance limit of the joints 22%.
- After fatigue tests, when failure surfaces were examined, the failure mode of unreinforced joints and nano-$Al_2O_3$ reinforced joints were obtained to be interfacial at the lower maximum loads, however, at bigger maximum loads, it can be seen that the failure was mixed type (interfacial and cohesive).

- After fatigue tests, the failure mode of nano-$TiO_2$ and $SiO_2$ reinforced joints was generally obtained to be interfacial both the lower maximum loads and bigger maximum loads.

Since the fatigue tests took a long time, the mixing ratios of the nanoparticles added into the adhesive were fixed. These values were taken as the ratios of the highest damage loads obtained in the tensile tests and compared with the neat adhesive samples. In subsequent studies it will be useful to experiment with varying nanoparticle mixture ratios.

## Acknowledgements

We are grateful to Batman University Scientific Research Projects (BAP) Coordinator for providing financial support for the realization of our work **(Project number: BTÜBAP-2016-PhD-2).** And also we would like to thank to Ihsan Pilatin, the lecturer of English at Batman University, for his preliminary contributions in correcting of grammar faults.

## References

[1] Ünal E. Simulation of fatigue of glass fiber composite materials in atmospheric environment and sea environment. Graduate Thesis. Ege University Institute of Science and Technology, İzmir:2006.

[2] Çitil Ş, Ayaz Y and Temiz Ş. Stress analysis of adhesively bonded double strap joints with or without intermediate part subjected to tensile loading. The Journal of Adhesion 2017;93(5):343-356.

[3] Özel A, Yazıcı B, Akpınar S, Aydın MD and Temiz Ş. A study on the strength of adhesively bonded joints with different adherends. Composites Part B: Engineering 2014;62:167-174.

[4] Çitil Ş. Comparison of Stepped, Curved, and S-Type Lap Joints Under Tensile Loading. In: Lucas F. M. da Silva, editor. Materials Design and Applications. Porto: Springer, 2017. p.377-388.

[5] Gültekin K, Akpınar S and Özel A. The effect of the adherend width on the strength of adhesively bonded single-lap joint: Experimental and numerical analysis. Composites Part B: Engineering 2014;60:736-745.

[6] Çitil Ş, Ayaz Y, Temiz Ş and Aydın MD. Mechanical behaviour of adhesively repaired pipes subject to internal pressure. International Journal of Adhesion and Adhesives 2017;75:88–95.

[7] Çitil S¸ Temiz S, Altun H and Özel A. Determination of Mechanical Properties of Double-Strap Adhesive Joints with an Embedded Patch. Journal of Adhesion Science and Technology 2011;25:2555–2567.

[8] Ghosh PK, Kumar K, Preeti P, Rajoria M and Misra N. Superior dissimilar adhesive joint of mild steel and aluminium using UDM processed epoxy based TiO2 nano-filler composite adhesive. Composites Part B: Engineering 2016;99:224-234.

[9] Gültekin K, Akpınar S, Gürses A, Eroğlu Z and Özel A. The effects of graphene nanostructure reinforcement on the adhesive method and the graphene reinforcement ratio on the failure load in adhesively bonded joints. Composites Part B: Engineering 2016;98:362-369.

[10] Akpınar IA, Gültekin K, Akpınar S, Akbulut H and Özel A. Experimental analysis on the single-lap joints bonded by a nanocomposite adhesives which obtained by adding nanostructures. Composites Part B: Engineering 2017;110:420-428.

[11] Ekrem M, Avcı A. Effects of polyvinyl alcohol nanofiber mats on the adhesion strength and fracture toughness of epoxy adhesive joints. Composites Part B: Engineering 2018;138:256-264.

[12] Meguid SA, Sun Y. On the tensile and shear strength of nano-reinforced composite interfaces. Materials and Design 2004;25: 289–296.

[13] Zhai L, Ling G, Li J, Wang Y. The effect of nanoparticles on the adhesion of epoxy adhesive. Materials Letters 2006; 60:3031–3033.

[14] Srivastava VK. Effect of carbon nanotubes on the strength of adhesive lap joints of C/C and C/C–SiC ceramic fibre composites. International Journal of Adhesion & Adhesives 2011;31:486-489.

[15] Mactabi R., Rosca LD, Hoa SV. Monitoring the integrity of adhesive joints during fatigue loading using carbon nanotubes. Composites Science and Technology 2013;78:1-9.

[16] Kang MH, Choi JH, Kweon JH. Fatigue life evaluation and crack detection of the adhesive joint with carbon nanotubes. Composite Structures 2014;108:417–422.

[17] Khashaba UA, Aljinaidi AA, Hamed, MA. Development of CFRE composite scarf adhesive joints with SiC and $Al_2O_3$ nanoparticle. Composite Structures 2015;128:415-427.

[18] Akpınar S. Experimental determination of the mechanical properties of the adhesives joints reinforced bonded with aluminum oxide and titanium dioxide. Niğde University Journal of Engineering Sciences 2016;5(2):244-252.

[19] Khashaba UA, Aljinaidi AA, Hamed MA. Fatigue and reliability analysis of nano-modified scarf adhesive joints in carbon fiber composites. Composite Part B 2017;1201:03-117.
[20] Akpınar IA, Gültekin K, Akpınar S, Akbulut H, Ozel A. Research on strength of nanocomposite adhesively bonded composite joints. Composite Part B 2017;126:143-152.
[21] Razavi SMJ, Ayatollahi MR, Nemati Giv A, Khoramishad H. Single lap joints bonded with structural adhesives reinforced with a mixture of silica nanoparticles and multi walled carbon nanotubes. International Journal of Adhesion & Adhesives 2018;80:76–86.
[22] Akpınar S. Effects of laminate carbon/epoxy composite patches on the strength of double-strap adhesive joints: Experimental and numerical analysis. Materials and Design 2013;51:501–512.
[23] Anonymous, https://bircelik.com/tr/category/stainless-steel, Visit date 5 May 2017.
[24] Anonymous, https://nanografi.com, Visit date 3 May 2017.
[25] Anonymous, https://3M.com/tr/structuraladhesives, Visit date 2 June 2017.
[26] Rudawska A. Pressure during curing and the strength of 2024, 2017A and 1050 aluminum alloy sheet adhesive joints. Advances in Science and Technology Research Journal 2015;9:96-103.
[27] Khashaba UA, Najjar IMR. Adhesive layer analysis for scarf bonded joint in CFRE composites modified with MWCNTs under tensile and fatigue loads, Composite structures 2018;184:411-427.
[28] Zhai L, Ling G, Wang Y. Effect of Nano-$Al_2O_3$ on Adhesion Strength of Epoxy Adhesive and Steel. International Journal of Adhesion & Adhesives 2007;28:23-28.
[29] Khoramishad H, Crocombe AD, Katnam KB, Ashcroft IA. A generalized damage model for constant amplitude fatigue loading of adhesively bonded joints, International Journal of Adhesion & Adhesives. 2010;30:513–521.

**Figure Captions**

**Fig. 1.** Single lap joint geometry

**Fig. 2.** The determination of adhesive and nanoparticle weight

**Fig. 3.** The application of adhesive to adherents

**Fig. 4.** The mold used in the preparation of the SLJs samples

**Fig. 5.** Molding in the production of samples

**Fig. 6.** Applying weight to samples

**Fig. 7.** The samples removed from the mold subsequent to curing process

**Fig. 8.** The boundary conditions the SLJs

**Fig. 9.** Shimadzu AG-I (250 kN) tensile test device

**Fig. 10.** 100 kN computer controlled Shimadzu EHF-EV universal fatigue device

**Fig. 11.** Average failure loads of the SLJs reinforced by nano-$Al_2O_3$, nano-$TiO_2$ and nano-$SiO_2$

**Fig. 12.** Load-displacement curves of the joints

**Fig. 13.** Fracture surfaces of the SLJs (a-unreinforced, b-reinforced by $Al_2O_3$, c-reinforced by $TiO_2$, d-reinforced by $SiO_2$)

**Fig. 14.** S-N curves of the SLJs (a-reinforced by $Al_2O_3$/unreinforced, b-reinforced by $TiO_2$/unreinforced, c-reinforced by $SiO_2$/unreinforced)

**Fig. 15.** Crack length variation of the adhesive joint [6].

**Fig.16.** Fractured surfaces of the SLJs produced with neat adhesive (a-Pmax: 3,69 kN, b-Pmax: 3,17 kN, c-Pmax: 2,64 kN)

**Fig.17.** Fractured surfaces of the SLJs reinforced by nano-$Al_2O_3$ (a-$P_{max}$: 4,22 kN, b-$P_{max}$: 3,69 kN, c-$P_{max}$: 3,17 kN)

**Fig.18**. Fractured surfaces of the SLJs reinforced by nano-$TiO_2$ (a-$P_{max}$: 3,17 kN, b-$P_{max}$: 2,64 kN, c-$P_{max}$: 2,13 kN)

**Fig.19**. Fractured surfaces of the SLJs reinforced by nano-$SiO_2$ (a-$P_{max}$: 3,17 kN, b-$P_{max}$: 2,90 kN, c-$P_{max}$: 2,67 kN)

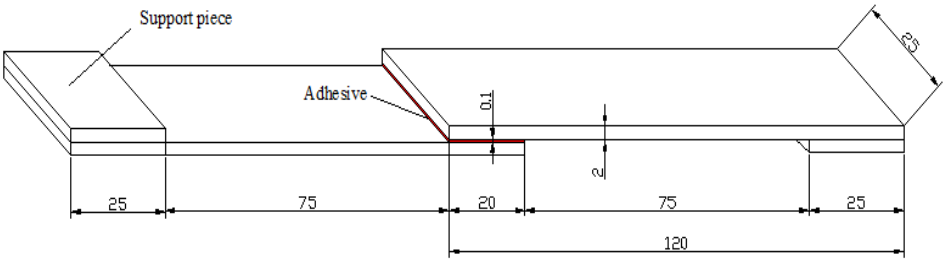


Fig. 1.

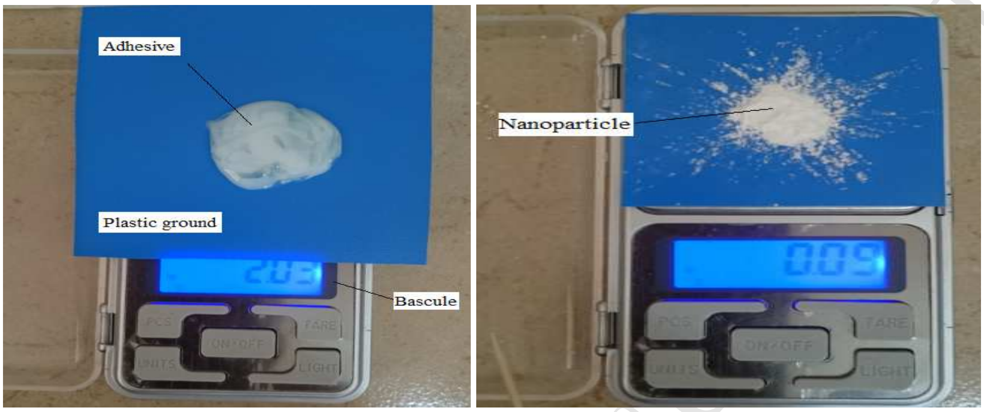


Fig. 2.

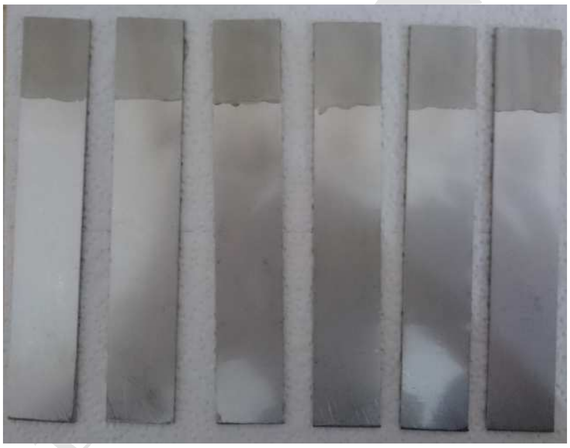

Fig. 3.

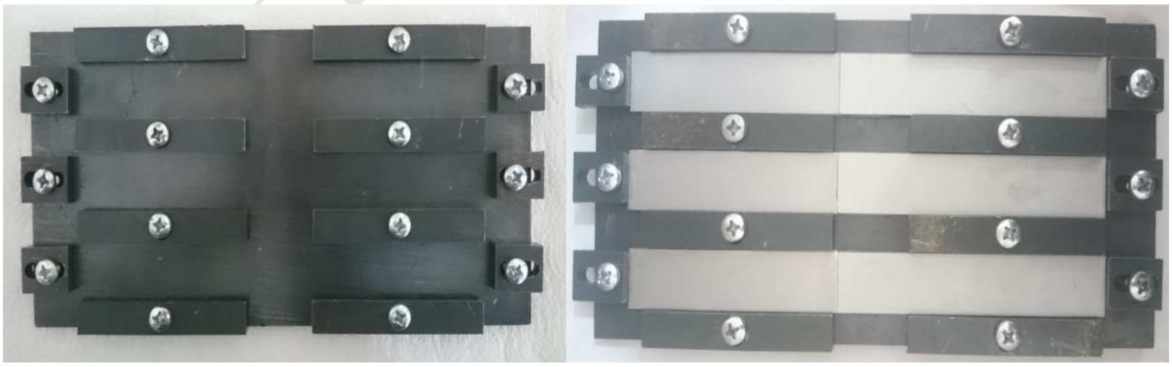

Fig. 4.

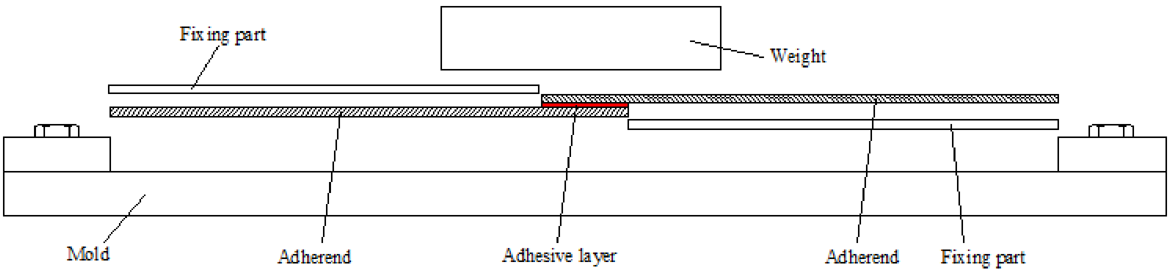


**Fig. 5.**

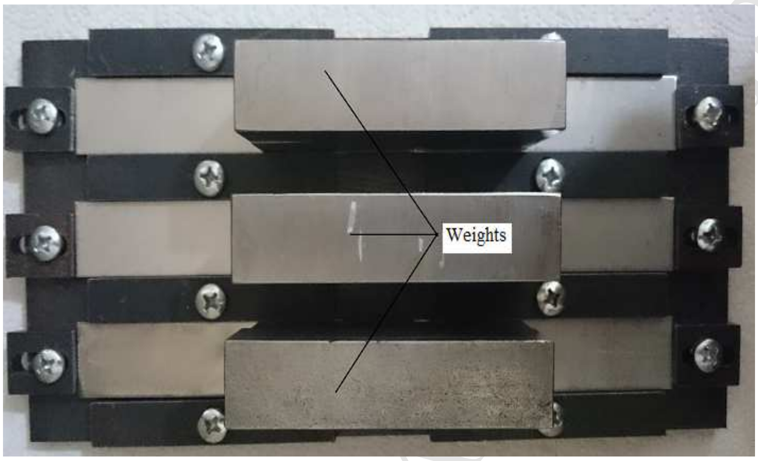


**Fig. 6.**

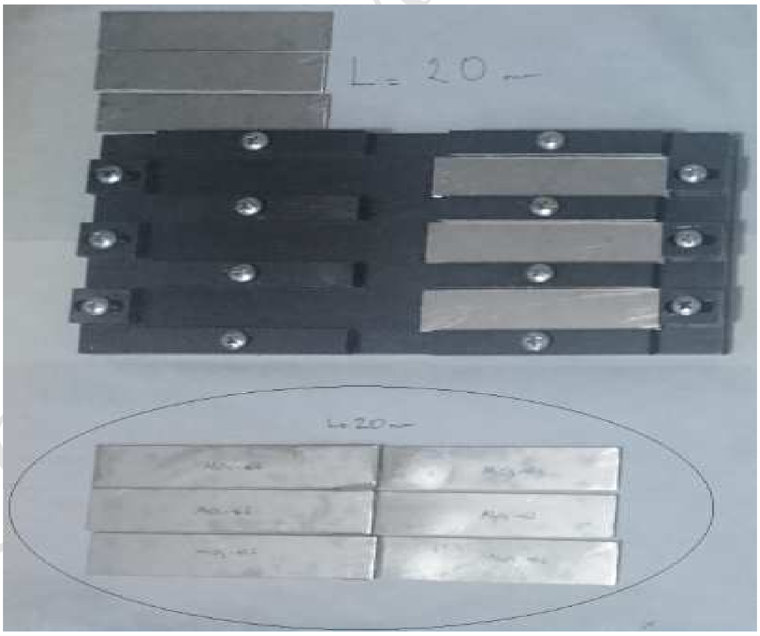

**Fig. 7.**

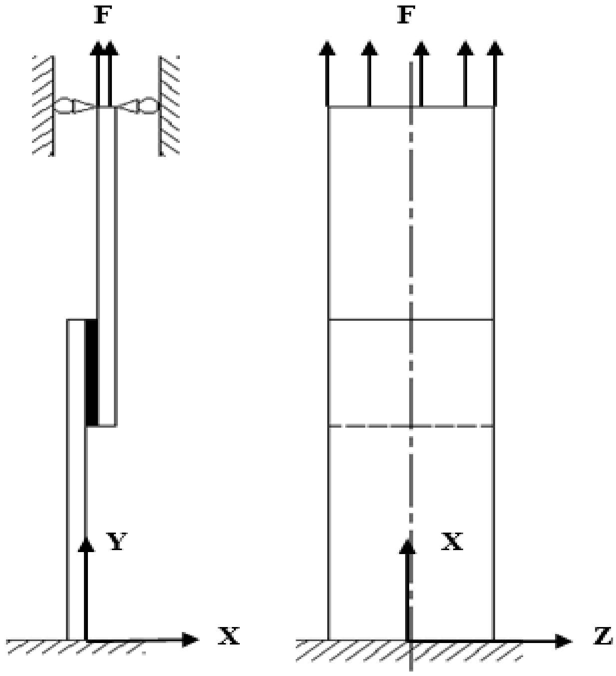


**Fig.8.**

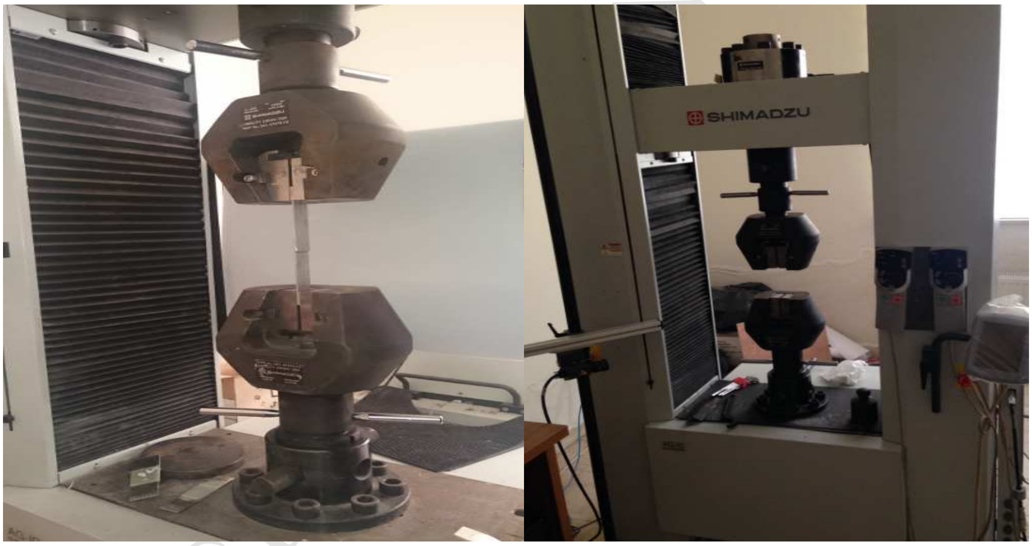


**Fig. 9.**

**Fig. 10.**

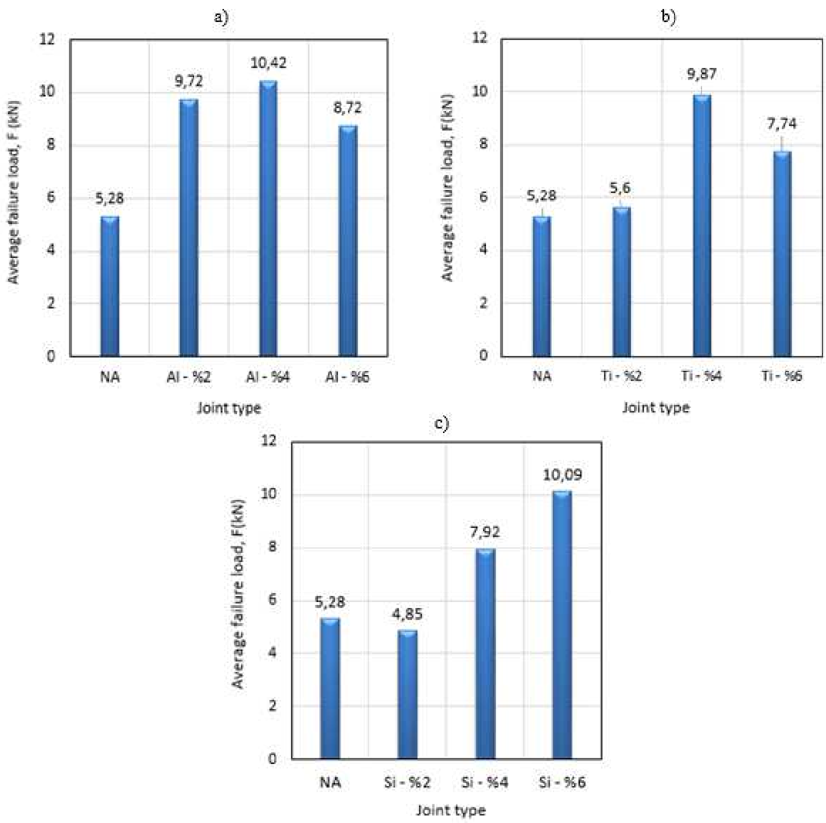
a)
Average failure load, F (kN)
5,28
9,72
10,42
8,72
NA
Al - %2
Al - %4
Al - %6
Joint type
b)
Average failure load, F(kN)
5,28
5,6
9,87
7,74
NA
Ti - %2
Ti - %4
Ti - %6
Joint type
c)
Average failure load, F(kN)
5,28
4,85
7,92
10,09
NA
Si - %2
Si - %4
Si - %6
Joint type

**Fig. 11.**

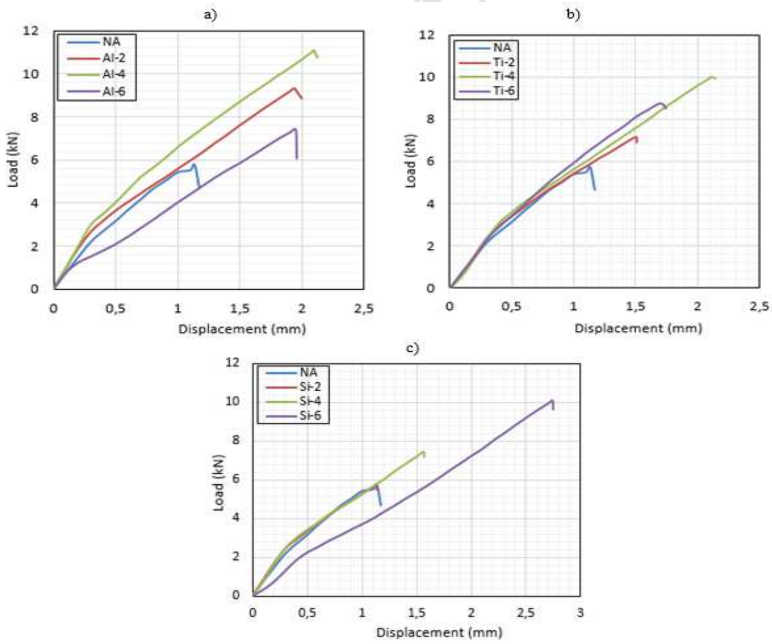
a)
NA
Al-2
Al-4
Al-6
Load (kN)
Displacement (mm)
b)
NA
Ti-2
Ti-4
Ti-6
Load (kN)
Displacement (mm)
c)
NA
Si-2
Si-4
Si-6
Load (kN)
Displacement (mm)

**Fig. 12.**

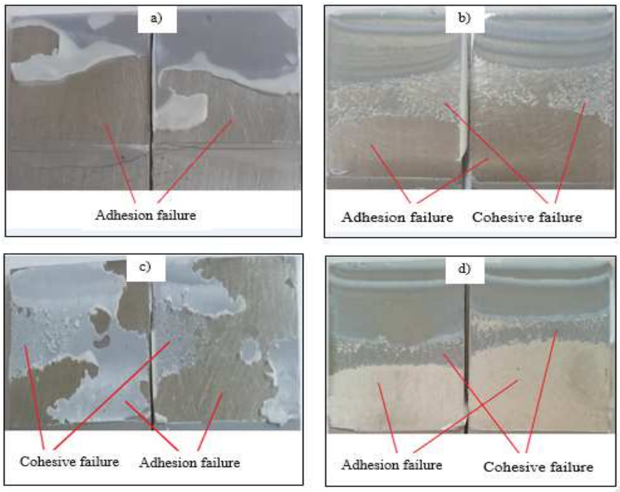

a)
Adhesion failure
b)
Adhesion failure
Cohesive failure
c)
Cohesive failure
Adhesion failure
d)
Adhesion failure
Cohesive failure


**Fig. 13.**

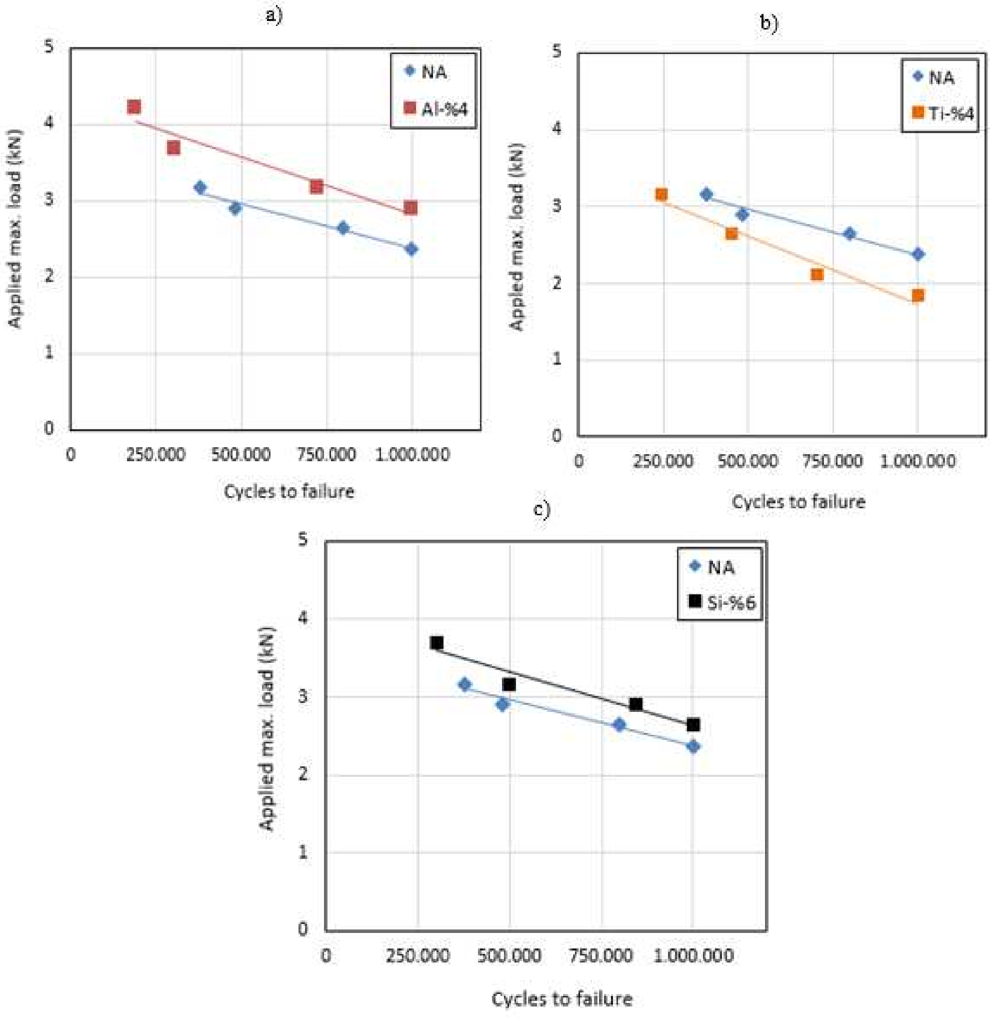

a)
Applied max. load (kN)
Cycles to failure
NA
Al-%4
0
250.000
500.000
750.000
1.000.000
b)
Applied max. load (kN)
Cycles to failure
NA
Ti-%4
c)
Applied max. load (kN)
Cycles to failure
NA
Si-%6


**Fig. 14.**

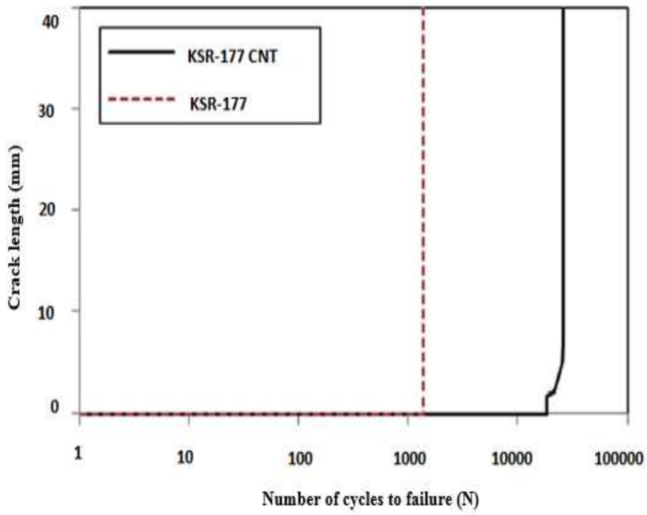


**Fig. 15.**

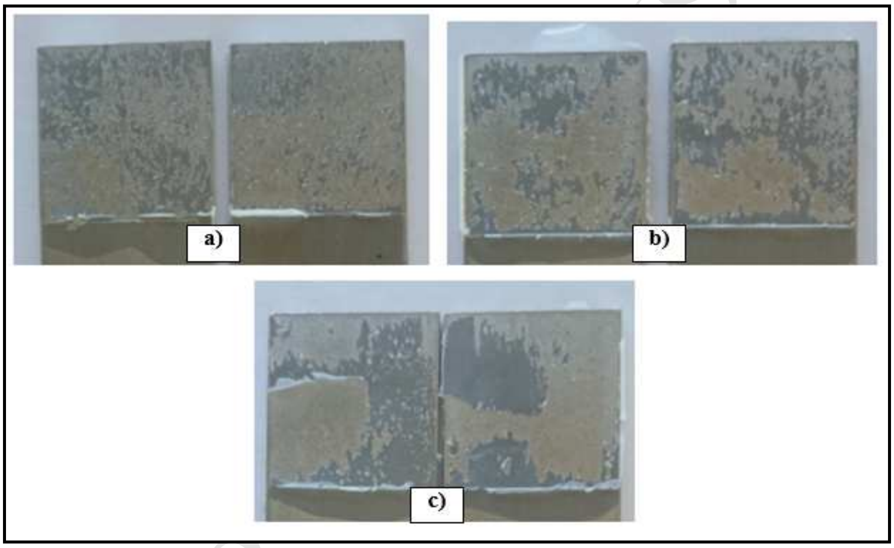


**Fig.16**.

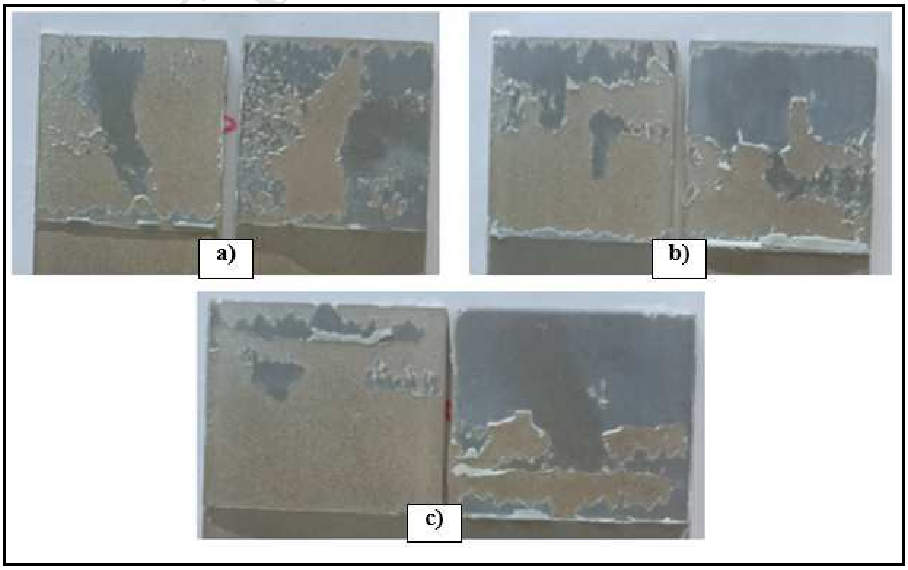


**Fig.17**.

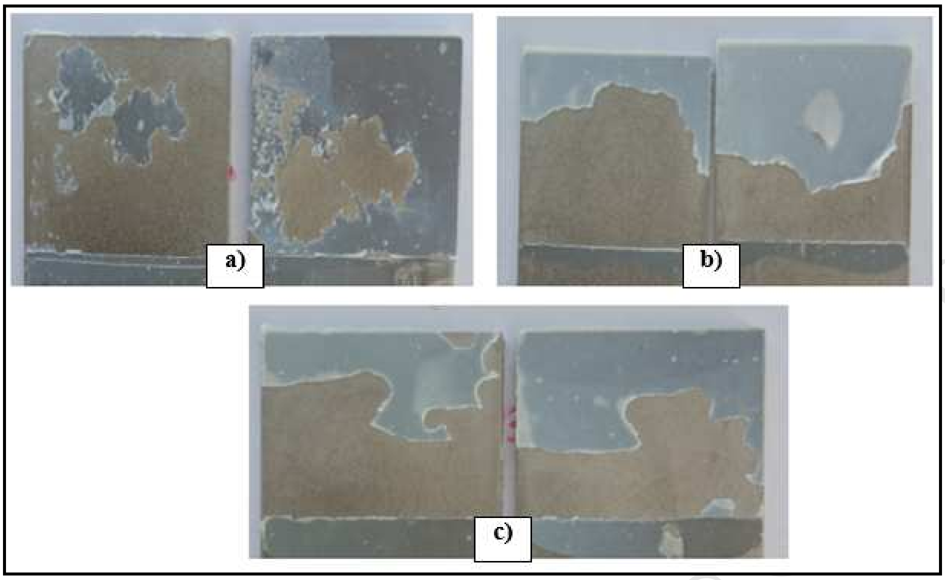


**Fig.18**.

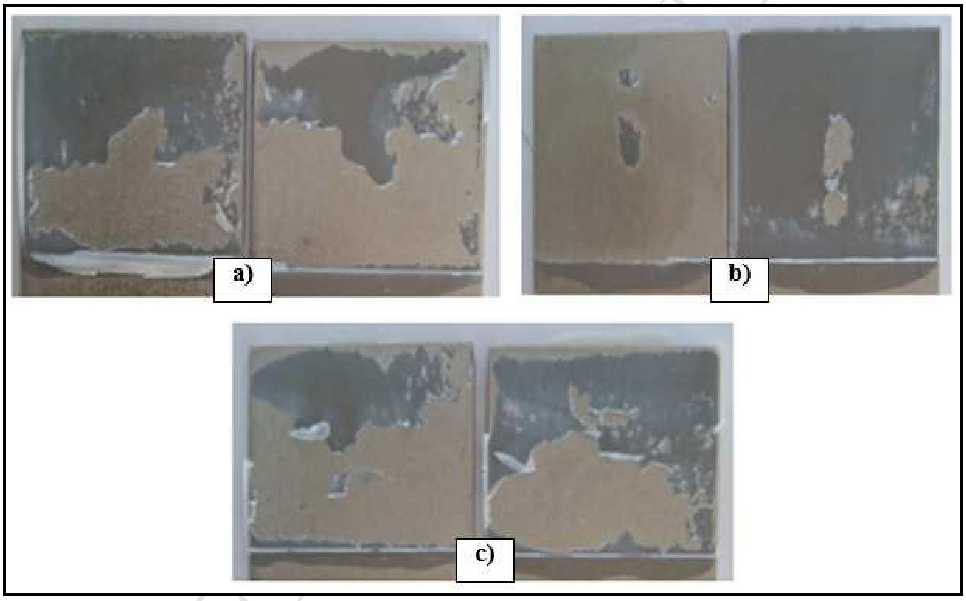


**Fig.19**.

**Table captions**

**Table 1** Material properties of the adhesive [22].
**Table 2** Material properties of the adherend [23].
**Table 3** Properties of the nanoparticles [24].
**Table 4** Curing condition and mixing ratio of the DP460 [25].
**Table 5** Joint and particle types for fatigue tests
**Table 6** Joint types for fatigue tests
**Table 7** The maximum failure loads and the weight percentages of the nanoparticles

**Table 1** Material properties of the adhesive [22].

| | |
|---|---|
| $\sigma_t$ (MPa) | 38.4 ± 1.1 |
| E (MPa) | 1984 ± 43 |
| $\upsilon$ | 0,37 |
| $\varepsilon_t$ (%) | 4.7 |

$\sigma_t$: Ultimate tensile strength; E: Young's modulus; $\upsilon$: Poisson's ratio; $\boldsymbol{\varepsilon_t}$: Ultimate tensile strain

**Table 2** Material properties of the adherend [23].

| | |
|---|---|
| $\sigma_t$ (MPa) | 515-720 |
| $\sigma$ (MPa) | 210 |
| E (GPa) | 190 |
| $\upsilon$ | 0.29 |
| $\boldsymbol{\varepsilon_t}$ (%) | ≥50 |

$\sigma_t$: Ultimate tensile strength; $\sigma$: Yield strength (MPa); E: Young's modulus; $\upsilon$: Poisson's ratio; $\boldsymbol{\varepsilon_t}$: Ultimate tensile strain

**Table 3** Properties of the nanoparticles [24].

| | $Al_2O_3$ | $TiO_2$ | $SiO_2$ |
|---|---|---|---|
| Average particle size (nm) | 20 | 10-25 | 15-20 |
| Specific surface area ($m^2$/g) | 140 | 60 | 150-550 |
| Density(kg/$m^3$) | 3900 | 4100 | 2200 |
| Purity (%) | 99 | 99 | 99,5 |

**Table 4** Curing condition and mixing ratio of the DP460 [25].

| | Mixing ratio (Epoxy: A/Hardener:B) | Curing temperature/time |
|---|---|---|
| 3M™ DP 460 | A:B = 2:1 | 23 $^0$C/24 hour |

**Table 5** Joint and particle types for fatigue tests

| Joint type | Nanoparticle type | The weight ratio of the nanoparticle in the adhesive (%) |
|---|---|---|
| NA | Neat adhesive | - |
| Al-2 | $Al_2O_3$ | % 2 |
| Al-4 | $Al_2O_3$ | % 4 |
| Al-6 | $Al_2O_3$ | % 6 |
| Ti-2 | $TiO_2$ | % 2 |
| Ti-4 | $TiO_2$ | % 4 |
| Ti-6 | $TiO_2$ | % 6 |

| | | |
|---|---|---|
| Si-2 | $SiO_2$ | % 2 |
| Si-4 | $SiO_2$ | % 4 |
| Si-6 | $SiO_2$ | % 6 |

NA: Neat adhesive; Al: $Al_2O_3$; Ti: $TiO_2$; Si: $SiO_2$

**Table 6** Joint types for fatigue tests

| Joint type | Nanoparticle type | The weight ratio of the nanoparticle in the adhesive (%) |
|---|---|---|
| NA | Neat adhesive | - |
| Al-4 | $Al_2O_3$ | % 4 |
| Ti-4 | $TiO_2$ | % 4 |
| Si-6 | $SiO_2$ | % 6 |

NA: Neat adhesive; Al: $Al_2O_3$; Ti: $TiO_2$; Si: SiO

**Table 7** The maximum failure loads and the weight percentages of the nanoparticles

| Joint type | Max. failure load (F, kN) | The weight ratio of the nanoparticle in the adhesive (%) |
|---|---|---|
| Al-4 | 10.42 | % 4 |
| Ti-4 | 9.87 | % 4 |
| Si-6 | 10.09 | % 6 |

Al: $Al_2O_3$; Ti: $TiO_2$; Si: $SiO_2$

**HIGHLIGHTS**

Behavior of nano-particle used in the adhesive joints was analyzed as experimental.

The effects of nano-particles were investigated in the single lap joints on the static and fatigue strength.

Three type nano-particles are used to mix with adhesive.

The highest average failure load was obtained with 4wt% nano-$Al_2O_3$ in epoxy adhesive.

It was observed that the addition of the nano-$Al_2O_3$ and nano-$SiO_2$ to the adhesive increased fatigue strength of the adhesive joints.